Quantum Electronics **41** (2) 179 – 184 (2011)

IMAGE FORMATION

PACS numbers: 42.25.Kb; 42.30.Ms; 42.30.Wb
DOI: 10.1070/QE2011v041n02ABEH014348

Use of a temporal approach to the three-dimensional image formation of a distant rough nonplanar object

V.I. Mandrosov

***Abstract*. A method is proposed to reconstruct three-dimensional images of a distant nonplanar rough object by the speckle pattern of its flat image, which is calculated using the temporal approach based on the time correlation function of probe radiation with a coherence length smaller than the size of the probed object. We analyse the influence of the angular resolution of the optical system, forming an image of the object, and additive noises on the reconstruction accuracy of the object surface shape using the proposed method.**

Keywords: *optical coherence, three-dimensional objects of distant rough objects, speckle pattern in optical images.*

1. Introduction

The literature describes several methods for forming three-dimensional images of distant rough nonplanar objects. The methods are based on digital processing of the intensity distribution in the flat images [1 – 4]. They include, for example, actively adopted methods of three-dimensional imaging, implemented by processing the intensity distributions in two flat images (stereo pairs) of the object obtained from two perspectives [2, 3]. The relevance of these methods is associated with their use for solving a wide range of problems, including the problems of determining the shape of the distant objects in order to significantly increase the probability of their recognition; of high-precision reconstruction of the topography of the Earth's surface, especially in mountainous terrains, by the results of its aerial survey [2]; and of obtaining laser-induced three-dimensional images of objects in transparent crystals [3]. However, the implementation of these methods is time-consuming and, in the case of far distant objects, requires a sufficiently large separation of the optical axes of the receiving optical systems generating these two images. In particular, Troitsky [3] proposed a method for reconstructing the shape of the object surface, i.e., three-dimensional imaging of the object by its two flat images generated when the axes are arranged mutually perpendicular, which for far distant objects makes the implementation of this method virtually impossible.

In [4] we made an attempt to reconstruct a three-dimensional image of a distant rough nonplanar object by the contrast of the speckle pattern $C_k = C(\boldsymbol{\delta}_k)$ of the time-averaged intensity distribution $I_0(\boldsymbol{\delta}_k)$ in various (of the same shape) sites of its flat image, obtained in a single perspective, where $\boldsymbol{\delta}_k$ is the radius vector of the centre of the kth site. In this case, the shape of each site represents a square with sides equal to the average size of a speckle $\delta_r \approx z_i w$ [5], where $w = 0.61\lambda_0/d_\rho$ is the Rayleigh angular resolution [6] of the optical system that forms the image; $\lambda_0 = \omega_0/c$ is the average wavelength of probe radiation; z_i is the distance from the receiving aperture of the optical system forming the image to the image plane; d_ρ is the diameter of the receiving aperture.

Then, using a set of measured values C_k, the minimum resolvable sites of the object surface are approximated by parallelepipeds with the height of the kth parallelepiped $L_k \approx L_c/C_k$, where L_c is the coherence length of probe radiation. In this case, the base of the parallelepipeds is a square with the side $\Delta = wr_c$, where r_c is the distance between the receiving aperture and the probed object. However, we did not describe [4] the method allowing for the three-dimensional image reconstruction of a distant rough nonplanar object for the set of the C_k quantities by the position of approximating parallelepipeds in space. In this paper, we give a detailed description of this method, taking into account the effect of both the angular resolution w of the optical system that forms an image of a distant nonplanar object, and the additive noises on the reconstruction accuracy of the shape of the distant object surface.

2. Method for reconstructing three-dimensional images of distant objects with a temporal approach

Let us describe the proposed method (Fig. 1). The distant rough object (*1*) under study is probed by a small source of coherent radiation with a coherence length L_c that is smaller than the size of the object. The optical system (*3*) forms a flat image of object (*1*) outlined by contour (*4*), the image being projected on the matrix receiver (*5*) consisting of photodetectors whose receiving apertures have the shape of a square with the sides equal to δ_r. The radius vector of the centre of the receiving aperture of the kvth photodetector $\boldsymbol{\delta}_{kv}$ has components $\delta_x = k\delta_r$ and $\delta_y = v\delta_r$. In this case, the kvth photodetector registers the time-averaged intensity distribution in the image of the object under study

V.I. Mandrosov Moscow Institute of Physics and Technology (State University), Institutskii per. 9, 141700 Dolgoprudnyi, Moscow region, Russia; e-mail: vmandrosov@mail.ru

Received 26 April 2010; revision received 28 October 2010
Kvantovaya Elektronika **41** (2) 179 – 184 (2011)
Translated by I.A. Ulitkin

$$\bar{I}_0(\boldsymbol{\delta}_{kv}) = \frac{1}{T}\int_{t_0}^{t_0+T} I_0(\boldsymbol{\delta}_{kv})\mathrm{d}t,$$

where $I_0(\boldsymbol{\delta}_{kv}, t) = |E_0(\boldsymbol{\delta}_{kv}, t, \boldsymbol{\rho}_s)|^2$ is the instantaneous intensity in this image; t_0 and T is the initial time and time of its registration;

$$E_0(\boldsymbol{\delta}_{kv}, t, \boldsymbol{\rho}_s) \sim \frac{E_s}{\lambda_0 r_c}\int k(\boldsymbol{r})h(\boldsymbol{r}, \boldsymbol{\delta}_{kv}) \times \exp\left[-2\pi\mathrm{i}\,\frac{2r + \boldsymbol{r}\boldsymbol{\rho}_s/r_c + \xi(\boldsymbol{r})}{\lambda_0}\right] u\left(t - \frac{2r + \boldsymbol{r}\boldsymbol{\rho}_s/r_c}{c}\right)\mathrm{d}\boldsymbol{r} \quad (1)$$

is the instantaneous field at the receiving aperture of the kvth photodetector; $\boldsymbol{r}$ is the radius vector of a point on the object surface; $u(t)$ is the function of the probe radiation modulation [4] with the time correlation function

$$B_u(\tau) = \frac{1}{T}\int_{t_0}^{t_0+T} u(t)u^*(1+\tau)\mathrm{d}t;$$

$k(\boldsymbol{r})$ is the distribution of the reflection coefficients over the field on the surface of object (*1*); E_s and $\boldsymbol{\rho}_s$ are the field at the aperture and the radius vector of the probe radiation source; $\xi(\boldsymbol{r})$ is the distribution of heights of the surface roughnesses; $h(r, \boldsymbol{\delta}_{kv})$ is the pulse response of the optical system, forming an image. The registered signals $\bar{I}_0(\boldsymbol{\delta}_{kv})$ arrive to block (*6*), which reconstructs the shape of the object surface or, in other words, constructs a three-dimensional image of the object. Without loss of generality, we further assume that the optical axis of system (*3*) intersects the flat image of the probed object in the centre of gravity (the point O_i in Fig. 1). The orientation of the optical axis is defined by the unit vector $\boldsymbol{n}$ directed along the optical axis of system (*3*) toward the probed object.

The three-dimensional image of the object is reconstructed using a step approximation of the object surface by the system of parallelepipeds (Fig. 2). To do this, first with the temporal approach [4] based on the use of the function $B_u(\tau)$, we determined the contrast of the speckle pattern in a flat image on the kvth site of the image that is projected onto the receiving aperture of the kvth photodetector. In the absence of noise the contrast is determined by the formula [4]

$$C_{kv} = \frac{\langle \bar{I}_0^2(\boldsymbol{\delta}_{kv})\rangle_\xi}{\langle \bar{I}_0(\boldsymbol{\delta}_{kv})\rangle_\xi^2} - 1 \approx \frac{L_c}{L_{kv}}, \quad (2)$$

where $L_{kv} = L(\boldsymbol{\delta}_{kv})$ is the height of the parallelepiped approximating the site of the investigated object surface, that is optically conjugate with the kvth site of its image with its centre at the point with the radius vector $\boldsymbol{\delta}_{kv}$; angular brackets $\langle\ldots\rangle_\xi$ stand for averaging over different realisations of the heights of the surface roughnesses $\xi(\boldsymbol{r})$. Equation (2) is valid when $L_{kv} \geqslant 10L_c$ [4]. Then, in the plane XY, which is optically conjugate with the image plane $\delta_x\delta_y$, we construct grid (*2*) of square cells with the side $\Delta = \mu\delta_r = wr_c$, where $\mu = r_c/z_i$ is a scale factor. On this grid a closed line (*3*) is drawn, which repeats on a scale μ the contour of the flat image of the object [contour (*4*) in Fig. 1] and intersects the axes X and Y at points A′, B′, C′, D′, which correspond to the intersection points A, B, C, D

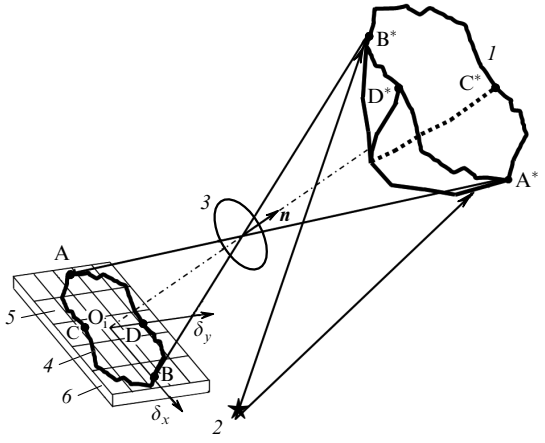

Figure 1. General scheme of registration of the intensity distribution in images of a distant nonplanar rough object and formation of its three-dimensional image: (*1*) the object of study; (*2*) a source of coherent radiation probing the object, (*3*) optical receiver producing a flat image of the probed object; (*4*) contour of the flat image of the object; (*5*) photodetector array; (*6*) generator of a three-dimensional image of the object; dash-and-dot line is the optical axis of receiving system (*3*); point O_i is the centre of gravity of the object image; points A*, B*, C*, D* are optically conjugate with the points A, B, C, D, located at the intersection of contour (*4*) with the coordinate axes δ_x, δ_y.

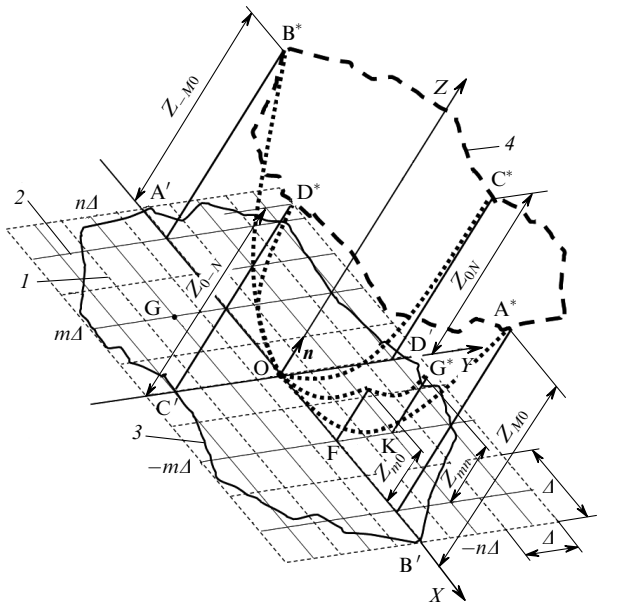

Figure 2. Scheme of reconstruction of arbitrary sites of the surface of the probed distant object at the scale $\mu = r_c/z_i$ in the coordinate system XYZ, oriented so that the plane XY is located parallel to the aperture of the photodetector array (*5*) in Fig. 1: (*1*) dashed grid reproducing at the scale μ the structure of the photodetector array (*5*) in Fig. 1; (*2*) coordinate grid on the plane XY; (*3*) closed line reproducing at the scale μ contour (*4*) in Fig. 1; (*4*) contour of the object (reconstructed at the scale μ) optically conjugate with the contour of its flat image (*4*) in Fig. 1; Z_{m0} and $Z_{mn} = \mathrm{KG}^*$ are the heights of surface sites of the reconstructed three-dimensional object image that are optically conjugate with sites of its image, projected on a photodetectors with the numbers $-m0$ and $-m-n$; Z_{-M0}, Z_{M0}, Z_{0N} and Z_{0-N} are the heights of the surface sites of the reconstructed three-dimensional object image that are optically conjugate with the sites of its flat image located near the intersection of points A, B, C, D of contour (*4*) in Fig. 1 with the axes δ_x and δ_y; dotted lines form the skeleton of the reconstructed surface of the object.

of the coordinate axes δ_x and δ_y with contour (*4*) in Fig. 1. Then, on grid (*2*) for $-m-n$th cell the point G is fixed with coordinates $x = -m\Delta$, $y = -n\Delta$, which corresponds to the centre of the $-m-n$th section of the flat image, whose radius vector has components $\delta_x = -m\delta_r$ and $\delta_y = -n\delta_r$. After that, on the reconstructed surface we determined the coordinates $x_0 = m\Delta$, $y_0 = n\Delta$ and $z_0 = Z_{mn}$ of the point G^* that is optically conjugate with the point G. Provided $L_{mn} \geqslant 10L_c$ and taking into account relations (2), the height of the mnth approximating parallelepiped KG^* with the lower square base, coinciding with the mnth cell of grid (*2*) (Fig. 2),

$$Z_{mn} = Z_{m0} + \sum_{v=0}^{n} L_{mv} \approx Z_{m0} + L_c \sum_{v=0}^{n} 1/C_{mv}, \tag{3}$$

where

$$Z_{m0} = \sum_{k=0}^{m} L_{k0} \approx L_c \sum_{k=0}^{n} 1/C_{k0} \tag{4}$$

is the height of the $m0$th approximating parallelepiped with upper square base whose point of intersection of the diagonals has coordinates $x_0 = m\Delta$, $y_0 = 0$ and $z_0 = Z_{m0}$. The Z_{m0} is calculated using formula (4) by summing the quantities L_{k0} along the segment OF on the axis X. To calculate Z_{mn} in accordance with formula (3) we performed additional summation of the quantities L_{mv} along the segment FK, parallel to the axis Y. The points A^*, B^*, C^*, D^* located on the contour of the image of the object surface at heights Z_{-M0}, Z_{M0}, Z_{0N}, Z_{0-N}, respectively (Fig. 2), are optically conjugate with the points A, B, C, D shown in Fig. 1. We will estimate these heights below.

Specifying the object surface as a function of $Z_0(x, y)$, we will show that with decreasing Δ the height of the mnth approximating parallelepiped Z_{mn} tends to the height of this surface $Z_0(x_0, y_0)$. In fact, from relations (3) and (4) we obtain

$$Z_{mn} = \sum_{k=0}^{m} L_{k0} + \sum_{v=0}^{n} L_{mv}, \tag{5}$$

where, as seen from geometrical assumptions,

$$L_{k0} = Z_{k0} - Z_{(k-1)0} \approx Z'_{0x}(x = k\Delta, 0)\Delta, \tag{6}$$

$$L_{mv} = Z_{mv} - Z_{m(v-1)} \approx Z'_{0y}(x = m\Delta, y = v\Delta)\Delta. \tag{7}$$

We assume below that $Z_0(0, 0) = 0$. Then, passing at $\Delta \to 0$ from summation in relation (5) to integration with account for (6) and (7), we obtain

$$Z_{mn} \to \int_0^{x_0} Z'_{0x}(x, 0)\mathrm{d}x + \int_0^{y_0} Z'_{0y}(x_0, y)\mathrm{d}y = Z_0(x_0, 0)$$

$$-Z_0(0, 0) + Z_0(x_0, y_0) - Z_0(x_0, 0) = Z_0(x_0, y_0), \tag{8}$$

which was to be proved.

Figure 3 shows a scheme illustrating the reconstruction of the object surface under study by its approximation by the system of parallelepipeds with square bases $\Delta \times \Delta$ in those of its parts, which are optically conjugate with the sites of the flat image of the object, located on the coordinate axes δ_x and δ_y. Parallelepipeds (*4*, *5*, *6*, *7*) with heights Z_{-M0}, Z_{M0}, Z_{0N}, and Z_{0-N} (Fig. 2) approximate the sites of the reconstructed surface, are optically conjugate with sites of flat image of the probed object centred at points A, B, C, D, which are located under the numbers $-M0$, $M0$, $0N$, $0-N$ at the intersection of the contour of image (*2*) with the axes δ_x and δ_y. The heavy dashed line and the dotted line in the image plane show the paths which are used in formula (4) to sum the quantities L_{k0} in order to determine the heights Z_{-M0} and Z_{M0} of the sites of the reconstructed surface which are optically conjugate with $-M0$th and $M0$th sites of the flat image centred at the points A and B, denoted by the radius vectors $\boldsymbol{\delta}_1$ and $\boldsymbol{\delta}_2$. Figure 3 also shows the radius vectors $\boldsymbol{r}_1$ and $\boldsymbol{r}_2$ of the points A^* and B^* on the reconstructed surface of the object, which are optical conjugate with points A and B. Similarly, we define the heights Z_{0N} and Z_{0-N}.

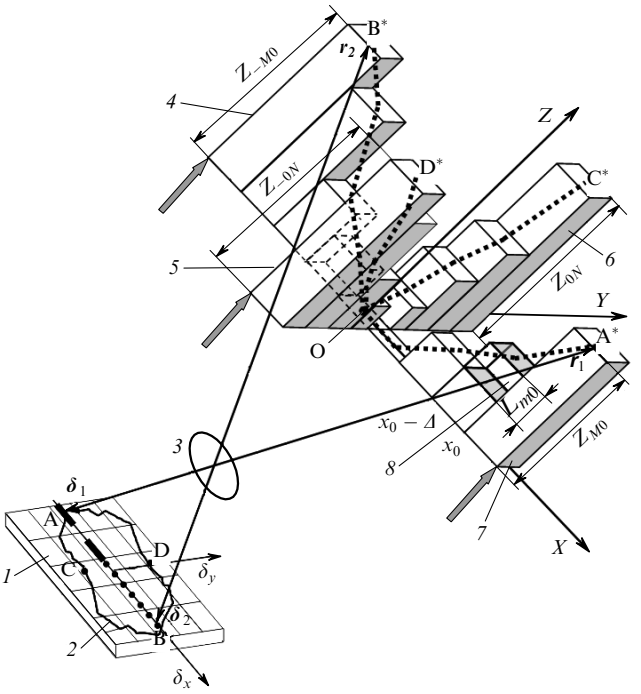

Figure 3. Scheme of the surface reconstruction of the probed object by its approximation by the system of parallelepipeds in those sites that are optically conjugate with the sites of the object image, located on the coordinate axes δ_x and δ_y: (*1*) aperture of the photodetector array; (*2*) contour of the flat image of the object; (*3*) optical system forming the image of the object; (*4–7*) parallelepipeds approximating the surface of the reconstructed three-dimensional image of the object in those of its sites, which are optically conjugate with the sites of the flat image of the object, located at the intersection of contour (*2*) with the axess δ_x and δ_y; (*8*) parallelepiped approximating the site of the object surface located between the points with the coordinates $x = x_0$ and $x = x_0 - \Delta$; dashed lines show the cross sections B^*OA^* and D^*OC^* of the reconstructed surface by mutually perpendicular planes XZ and YZ; arrows indicate the direction of the probe radiation with respect to the probed object.

3. Influence of the angular resolution of the optical system that forms images of a distant object on the reconstruction accuracy of the shape of its surface

The presented method allows one to construct a three-dimensional image of the object by approximating its surface by the system of parallelepipeds with square bases

$\Delta \times \Delta$ and heights, determined by the contrast of the speckle pattern in different parts of a flat image of the object. But this approximation for large $\Delta = wr_c$, i.e., with poor angular resolution w of the optical system (*3*) in Figs 1 and 3, is quite rough; as a result, the reconstructed shape of the object surface will have at different points (x_0, y_0) different deviations from its original form $\delta Z_0(x_0, y_0) = Z_0(x_0, y_0) - Z_{mn}$. Let us determine the reconstruction accuracy of the shape of the object surface at the point (x_0, y_0) as the relative error $\eta(x_0,y_0) = \delta Z_0(x_0,y_0) \times Z_0^{-1}(x_0,y_0)$ of the estimate of the height $Z_0(x_0, y_0)$. Without loss of generality, we estimate this error as a function of w under the assumption that $Z_0(x, y) = (x^2 + y^2)/(2a)$, where a is the radius of curvature of the surface, and that the height Z_{m0} is determined in the cross section B^*OA^* of the surface by the plane XZ (see Fig. 3) at the point with the coordinates $x = x_0,\ y = 0$. Given that this section is a parabola $Z_0(x, 0) = x^2/(2a)$, and with allowance for (4) we have

$$Z_{m0} = \sum_{k=0}^{m} L_{k0} \approx L_c \sum_{k=0}^{m} 1/C_{k0} \approx \Delta \sum_{k=0}^{m} Z'_{0x}(k\Delta, 0)$$

$$= \sum_{k=0}^{m} k\Delta^2/a = (\Delta^2/a)m(m-1). \qquad (9)$$

Taking into account the relations $Z_0(x, 0) = x^2/(2a)$, $\Delta = wr_c$, $x_0 \approx m\Delta$, (8) and (9), we obtain $\eta(x_0, 0) \approx \Delta/x_0 = wr_c/x_0$. As the angular resolution w decreases down to a certain value of w_m, the accuracy of determining the shape of the surface increases. This is due to the fact that η is reduced to the minimum error η_m of determining the height of the object surface at a point with the coordinates $x = x_0 = m\Delta$, $y = y_0 = 0$. In fact, it follows from (7) that the last term in (9) has the form $L_{m0} \approx x_0 wr_c/a$. This term defines the height of parallelepiped (*8*) in Fig. 3, approximating the site of the surface of the object, located between the points with coordinates $x = x_0 - \Delta,\ y = 0,\ z = Z_0(x_0 - \Delta, 0)$ and $x = x_0,\ y = 0,\ z = Z_0(x_0, 0)$. Note also that the relation $L_{m0} \approx x_0 wr_c/a$ takes place only when the condition $L_{m0} \geqslant 10L_c$ is met [4]. This condition implies that the angular resolution w should not be less than

$$w_m = 10L_c a/(r_c x_0)\,. \qquad (10)$$

Then, from the relation $\eta \approx wr_c/x_0$ we obtain

$$\eta_m \approx 10L_c a/x_0^2. \qquad (11)$$

When approaching the object surface top, located at a point with the coordinates $x = x_0 = 0$, $y = y_0 = 0$ (point O in Figs 2 and 3), the quantity η_m increases beyond all bounds. Therefore, it is expedient, for example, to select (around this top) a small region of radius $0.1a$ and high enough ($\eta_m = 0.05$) reconstruction accuracy of surface shape at the boundary of this site. Then, taking (10) and (11) into account, we get $w_m = 5 \times 10^{-3} a/r_c$. With this angular resolution outside the selected site, i.e., at $x_0 > 0.1a$, we have $\eta(x_0, 0) \approx w_m r_c/x_0$. As x_0 increases, η decreases, reaching a minimum $\eta_b \approx 5 \times 10^{-3}\sigma_\xi/l_\xi$ on the boundary of the site (radius $\rho_b = a\sigma_\xi/l_\xi$) of the backscattering of the object [7], where l_ξ and σ_ξ is the correlation radius and root-mean-square deviation of the heights of the roughnesses on the object surface. When the roughnesses of the object surfaces are smooth ($\sigma_\xi/l_\xi \approx 0.2$), $\eta_b \approx 10^{-2}$, and when they are steep ($\sigma_\xi/l_\xi \approx 1$), $\eta_b \approx 5 \times 10^{-3}$.

Thus, we have shown that there exists a minimal angular resolution w_m, at which the most accurate approximation of the object surface shape by the system of parallelepipeds is achieved. However, at a sufficiently high level of noises, even at such an angular resolution, the surface shape is reconstructed with visible distortions, the analysis of which will be given in Section 4.

4. Influence of additive noises on the reconstruction accuracy of the surface shape

We will analyse the effect of the additive noise field on the reconstruction accuracy of the surface of the object shape by the contrast of the time-averaged intensity distribution in its flat image. In the presence of noises, taking into account relation (1), the kvth photodetector (see Figure 1) detects the signal

$$\bar{I}_s(\boldsymbol{\delta}_{kv}) = \frac{1}{T}\int_{t_0}^{t_0+T} I_s(\boldsymbol{\delta}_{kv}, t)\mathrm{d}t,$$

where

$$I_s(\boldsymbol{\delta}_{kv}, t) = E_s(\boldsymbol{\delta}_{kv}, t, \boldsymbol{\rho}_s)|^2;$$

$$E_s(\boldsymbol{\delta}_{kv}, t, \boldsymbol{\rho}_s) = E_0(\boldsymbol{\delta}_{kv}, t, \boldsymbol{\rho}_s) + E_n(\boldsymbol{\delta}_{kv}, t);$$

$E_n(\boldsymbol{\delta}_{kv}, t)$ is the additive noise field at the receiving aperture of the photodetector. This field, as shown in [7], can be interpreted as a field in the image of a background, averagely flat, rough object mentally located near the distant object under study. Then, the contrast of the speckle pattern on the kvth site of the overall flat image of the studied and background objects $C_{skv} = \langle\langle \bar{I}_s(\boldsymbol{\delta}_{kv})^2\rangle_\xi\rangle_\zeta / \langle\langle \bar{I}_s(\boldsymbol{\delta}_{kv})\rangle_\xi\rangle_\zeta^2 - 1$, where the brackets $\langle \ldots \rangle_\zeta$ refer to the operation of averaging over the distribution of heights $\zeta(\boldsymbol{r})$ of surface roughnesses of background objects, performed along with the operation of averaging over the distribution $\xi(\boldsymbol{r})$. Assuming that the fields $E_0(\boldsymbol{\delta}_{kv}, t)$ and $E_n(\boldsymbol{\delta}_{kv}, t)$ are distributed by a Gaussian law and statistically independent, we obtain for the contrast C_{skv} the relationship:

$$C_{skv} = \left\{ \frac{1}{T^2}\int_{t_0}^{t_0+T}\int_{t_0}^{t_0+T} \left[|\langle E_0(\boldsymbol{\delta}_{kv}, t_1)E_0^*(\boldsymbol{\delta}_{kv}, t_2)\rangle_\xi|^2 + \right.\right.$$

$$\left.\left. + |\langle E_n(\boldsymbol{\delta}_{kv}, t_1)E_n^*(\boldsymbol{\delta}_{kv}, t_2)\rangle_\zeta|^2\right]\mathrm{d}t_1\mathrm{d}t_2 \right\} / F_{kv}^2, \qquad (12)$$

where

$$F_{kv} = \langle \bar{I}_0(\boldsymbol{\delta}_{kv})\rangle_\xi + \langle \bar{I}_n(\boldsymbol{\delta}_{kv})\rangle_\zeta;$$

$$\bar{I}_n(\boldsymbol{\delta}_{kv}) = \frac{1}{T}\int_{t_0}^{t_0+T} |E_n(\boldsymbol{\delta}_{kv}, t)|^2\mathrm{d}t$$

is the function, which can be interpreted as the time-averaged intensity distribution in the image of the background object. As follows from [7], when the angular resolution w of the optical system forming an image of the object is sufficiently high,

$$\langle \bar{I}(\boldsymbol{\delta}_{kv})\rangle_{\xi} \sim \int k_0(\boldsymbol{r})|h(\boldsymbol{r},\boldsymbol{\delta}_{kv})|^2 \mathrm{d}\boldsymbol{r} \approx \Delta^2 k_0(\boldsymbol{r}=-\mu\boldsymbol{\delta}_{kv}), \quad (13)$$

where

$$k_0(\boldsymbol{r}) \sim (l_\xi/\sigma_\xi)^2|k(\boldsymbol{r})|^2 \exp\left[-(q_\xi l_\xi/\sigma_\xi)^2\right] \quad (14)$$

is the intensity distribution of the reflection coefficient on the surface of the object under study; $q_\xi = q_\perp/q_N$; $q_\perp = (4-q_N^2)^{1/2}$; $q_N = \boldsymbol{q}\boldsymbol{N}$; $\boldsymbol{q} \approx 2\boldsymbol{r}/r$; $\boldsymbol{N}$ is the normal to the mean surface of the object. For the time-averaged intensity distribution $\bar{I}_\mathrm{n}$ in the image of the background object, we have an analogous relationship:

$$\langle \bar{I}_v(\boldsymbol{\delta}_{kv})\rangle_{\zeta} \sim \int k_\mathrm{n}(\boldsymbol{r})|h(\boldsymbol{r},\boldsymbol{\delta}_{kv})|^2 \mathrm{d}\boldsymbol{r}$$

$$\approx \Delta^2 (l_\zeta/\sigma_\zeta)^2 k_\mathrm{n}(\boldsymbol{r}=-\mu\boldsymbol{\delta}_{kv}), \quad (15)$$

where $k_\mathrm{n}(\boldsymbol{r})$ is the intensity distribution of the reflection coefficient on the surface of a background object; l_ζ and σ_ζ is the correlation radius and the root-mean-square deviation of the heights $\zeta(\boldsymbol{r})$ of the roughnesses on this surface.

Consider now the first term in curly brackets in (12), which, as follows from [4], after integration over t_1 and t_2 can be represented as

$$\frac{1}{T^2}\int_{t_0}^{t_0+T}\int_{t_0}^{t_0+T} |\langle E_0(\boldsymbol{\delta}_{kv},t_1)E_0^*(\boldsymbol{\delta}_{kv},t_2)\rangle_{\xi}|^2 \mathrm{d}t_1\mathrm{d}t_2$$

$$\approx \int\int k(\boldsymbol{r}_1)k(\boldsymbol{r}_2)|h(\boldsymbol{r}_1,\boldsymbol{\delta}_{kv})h^*(\boldsymbol{r}_2,\boldsymbol{\delta}_{kv})|^2 F(\boldsymbol{r}_1,\boldsymbol{r}_2)\mathrm{d}\boldsymbol{r}_1\mathrm{d}\boldsymbol{r}_2, \quad (16)$$

where $F(\boldsymbol{r}_1,\boldsymbol{r}_2) = |B_u[\tau/\tau_\mathrm{c} = (r_1-r_2)/L_\mathrm{c}]|^2$. We further assume that the condition $L_\mathrm{c} \ll L_{kv}$ is fulfilled. Taking into account this condition, the function $F(\boldsymbol{r}_1,\boldsymbol{r}_2)$ in expression (16) will be narrower than other functions, and after integration over $\boldsymbol{r}_1$, we obtain the relation:

$$\frac{1}{T^2}\int_{t_0}^{t_0+T}\int_{t_0}^{t_0+T} |\langle E_0(\boldsymbol{\delta}_{kv},t_1)E_0^*(\boldsymbol{\delta}_{kv},t_2)\rangle_{\xi}|^2 \mathrm{d}t_1\mathrm{d}t_2$$

$$\sim [L_\mathrm{c}/L_{kv}(\boldsymbol{\delta}_{kv})]\Delta^4 k_0^2(\boldsymbol{r}=-\mu\boldsymbol{\delta}_{kv}). \quad (17)$$

Taking into account that the background image is flat on average, we can show that the second term in the curly brackets in (12) has the form

$$\frac{1}{T^2}\int_{t_0}^{t_0+T}\int_{t_0}^{t_0+T} |\langle E_\mathrm{n}(\boldsymbol{\delta}_{kv},t_1)E_\mathrm{n}^*(\boldsymbol{\delta}_{kv},t_2)\rangle_{\zeta}|^2 \mathrm{d}t_1\mathrm{d}t_2$$

$$\sim (l_\zeta/\sigma_\zeta)^4 \Delta^2 k_\mathrm{n}^2(\boldsymbol{r}=-\mu\boldsymbol{\delta}_{kv}).$$

We assume below that $\sigma_\zeta/l_\zeta \approx 1$, i.e., the roughnesses of the background object surface have steep slopes. Then,

$$\frac{1}{T^2}\int_{t_0}^{t_0+T}\int_{t_0}^{t_0+T} |\langle E_\mathrm{n}(\boldsymbol{\delta}_{kv},t_1)E_\mathrm{n}^*(\boldsymbol{\delta}_{kv},t_2)\rangle_{\zeta}|^2 \mathrm{d}t_1\mathrm{d}t_2$$

$$\sim \Delta^2 k_\mathrm{n}^2(\boldsymbol{r}=-\mu\boldsymbol{\delta}_{kv}). \quad (18)$$

Finally, taking into account relations (12), (16), (17), and (18), we obtain

$$C_{\mathrm{s}kv} = \frac{[L_\mathrm{c}/L_{kv}(\boldsymbol{r}=-\mu\boldsymbol{\delta}_{kv})]k_0^2(\boldsymbol{r}=-\mu\boldsymbol{\delta}_{kv}) + k_\mathrm{n}^2(\boldsymbol{r}=-\mu\boldsymbol{\delta}_{kv})}{[k_0(\boldsymbol{r}=-\mu\boldsymbol{\delta}_{kv}) + k_\mathrm{n}(\boldsymbol{r}=-\mu\boldsymbol{\delta}_{kv})]^2}. \quad (19)$$

In the absence of noises, the height of the kvth parallelepiped with a base in the form of a square with the side $\Delta \approx \mu\delta_\mathrm{r}$, approximating the minimum resolvable kvth site of the object surface, is $L_{kv} \approx L_\mathrm{c}/C_{kv}$. The coordinates of the centre of the base in the coordinate system XYZ (Fig. 2) are related with the components δ_{xk} and δ_{yv} of the radius vector $\boldsymbol{\delta}_{kv}$ by the expressions $x_k = -\mu\delta_{xk}$, $y_v = -\mu\delta_{yv}$. In the presence of noises, the height of the kvth approximating parallelepiped is found from the relation $L_{\mathrm{s}kv} \approx L_\mathrm{c}/C_{\mathrm{s}kv}$. Provided $k_\mathrm{n}^2/k_0^2 \ll L_\mathrm{c}/L_{kv}$, i.e., for sufficiently small noises, taking into account expressions (13), (15) and (19) and under the assumption that noises are constant at different points of the image, namely $k_\mathrm{n}(\boldsymbol{r} = -\mu\boldsymbol{\delta}_{kv}) = k_\mathrm{n}(\boldsymbol{r}=0)$, we obtain the relationship:

$$L_{\mathrm{s}kv} - L_{kv} \approx \frac{2L_{kv}k_\mathrm{n}(0,0)}{k_0(x_k,y_v)} = \frac{2L_{kv}\langle \mathcal{I}_\mathrm{n}(\delta_{xk}=0,\delta_{yv}=0)\rangle_{\xi}}{\langle \mathcal{I}_0(x_k=-\mu\delta_{xk},y_v=-\mu\delta_{yv})\rangle_{\xi}}. \quad (20)$$

We will represent the object surface reconstructed in the presence of noises as a function of $Z(x,y)$ and fix in the XZ plane a point with the coordinates $x_0 = m\Delta$, $y_0 = n\Delta$ (Fig. 2). In the presence of additive noises, the height $Z(x_0,y_0)$ of the surface at this point is calculated from a formula, similar to (5), namely:

$$Z_{\mathrm{s}mn} = \sum_{k=0}^{m} L_{\mathrm{s}k0} + \sum_{v=0}^{n} L_{\mathrm{s}mv}. \quad (21)$$

Then, taking into account expressions (5)–(8), (19), and (21), from which it follows that

$$Z_{\mathrm{s}mn} - Z_{mn} \approx 2k_\mathrm{n}(0,0)$$

$$\times\left[\sum_{k=0}^{m} L_{k0}/k_0(x_k,0) + \sum_{v=0}^{n} L_{mv}/k_0(x_m,y_v)\right]$$

(Z_{mn} is the height of the mnth approximating parallelepiped in the absence of noises), at $\Delta \to 0$ we have

$$Z_{\mathrm{s}mn} - Z_{mn} \to 2k_\mathrm{n}(0,0)\left\{\int_0^{x_0} \frac{Z'_{0x}(x,0)}{k_0(x,0)}\,\mathrm{d}x + \right.$$

$$\left. + \int_0^{y_0} \frac{Z'_{0y}(x_0,y)}{k_0(x_0,y)}\,\mathrm{d}y\right\} \approx \delta Z(x_0,y_0), \quad (22)$$

where $Z(x_0,y_0) = Z(x_0,y_0) - Z_0(x_0,y_0)$. Taking into account (13)–(15), (21), and (22), we obtain

$$\delta Z(x_0,y_0) \approx 2\gamma_{\mathrm{n/s}}(\sigma_\xi/l_\xi)^2$$

$$\times\left\{\int_0^{x_0} Z'_{0x}(x,0)\exp[q_\xi(x,0)l_\xi/\sigma_\xi]^2\mathrm{d}x\right.$$

$$\left. + \int_0^{y_0} Z'_{0y}(x_0,y)\exp[q_\xi(x_0,y)l_\xi/\sigma_\xi]^2\mathrm{d}y\right\}, \quad (23)$$

where

$$\gamma_{n/s} = k_n(0,0)/k_0(0,0)$$

$$= \langle \bar{I}_n(\delta_{xk}=0,\delta_{yv}=0)\rangle_\zeta / \langle \bar{I}_0(\delta_{xk}=0,\delta_{yv}=0)\rangle_\xi .$$

This means that the coefficient $\gamma_{n/s}$ is equal to the ratio of the average intensity $\langle \bar{I}_n(\delta_{xk}=0,\delta_{yv}=0)\rangle_\zeta$ in the near-axial region in the image plane of the object under study in its absence to the average intensity $\langle \bar{I}_0(\delta_{xk}=0,\delta_{yv}=0)\rangle_\xi$ in the presence of the object and in the absence of noises. In the special case where the intensity of shot noises in the photodetector array (*5*) in Fig. 1 exceeds that of other noise, the quantity $\langle \bar{I}_n(\delta_{xk}=0,\delta_{yv}=0)\rangle_\zeta$ can be interpreted as their intensity. We will define the reconstruction accuracy of the object surface shape at the point (x_0, y_0) in the presence of noises as a relative error of $\eta_n(x_0,y_0) = \delta Z(x_0,y_0)/Z_0(x_0,y_0)$ of the estimate of the height $Z(x_0,y_0)$. On the assumption that this surface is fairly well approximated by a paraboloidal surface $Z_0(x,y) \approx x^2/(2a) + y^2/(2b)$, where a and b is the radius of its curvature, after integration over x and y in (23), we obtain

$$\eta_n(x_0,y_0) \approx \gamma_{n/s}(\sigma_\xi/l_\xi)^4 \frac{a(\exp X - 1) + b\exp X(\exp Y - 1)}{x_0^2/(2a) + y_0^2/(2b)},$$

where $X = [x_0 l_\xi/(\sigma_\xi a)]^2$; $Y = [y_0 l_\xi/(\sigma_\xi b)]^2$.

In particular, for a surface approximated by a paraboloid of revolution $Z_0(x,y) \approx (x^2+y^2)/(2a)$, we have

$$\eta_n(x_0,y_0) = \gamma_{n/s}(\sigma_\xi/l_\xi)^4 \frac{a^2\{\exp[\rho_0 l_\xi/(\sigma_\xi b)]^2 - 1\}}{\rho_0^2},$$

where $\rho_0 = (x_0^2 + y_0^2)^{1/2}$. At the boundary of the region (of radius $\rho_0 \approx \rho_b = a\sigma_\xi/l_\xi$) of the backscattering of the object under study $\eta_n = \eta_{n2} \approx \gamma_{n/s}(\sigma_\xi/l_\xi)^2(e-1) \approx 2\eta_{n1}$. Near the top of this surface ($x_0 = y_0 = 0$), when the condition $\rho_0 \ll \rho_b$ is met, $\eta_n = \eta_{n1} \approx \gamma_{n/s}(\sigma_\xi/l_\xi)^2$. From these results it is clear that the reconstruction accuracy of the object surface shape increases with increasing ρ_0, the coefficient $\gamma_{n/s}$ and the steepness σ_ξ/l_ξ of the slopes of the roughnesses of its surface, because in this case the angle of probe radiation scattering by each site of the surface increases, which leads to a decrease in the useful signal. In the case of steep slopes of the object surface roughnesses when $\sigma_\xi/l_\xi \approx 1$, we have $\eta_{n1} \approx \gamma_{n/s}$ and $\eta_{n2} \approx 2\gamma_{n/s}$. The relation $\eta_{n2} \approx 2\eta_{n1}$ means that when the ρ_0 approaches the boundary of the region (of radius $\rho_b \approx a\sigma_\xi/l_\xi$) of the object backscattering, the reconstruction accuracy of its surface decreases by about two times compared with that near the top surface of the nonplanar object under study. As in the case of steep slopes of the roughnesses $\eta_{n2} \approx 2\gamma_{n/s}$, then for the reconstruction accuracy of the shape of the object surface over the entire range of radii (from ρ_0 to ρ_b) to be, for example, below five percents, it is necessary that $\gamma_{n/s} \leqslant 0.025$.

5. Conclusions

Probing a distant nonplanar object by radiation with the coherence length smaller than the size of the object, the contrast speckle pattern of the flat image of the object can help reconstruct the shape of its surface, i.e., to form its three-dimensional image. In the absence of noises with decreasing the angular resolution of the optical system that forms the image of an object, the reconstruction accuracy of the surface shape of the object increases to a certain value w_m, because the estimation error of this shape is reduced to a minimum value η_m. However, at sufficiently high level of noises and at an angular resolution w_m, the surface shape is reconstructed inaccurately. In particular, in the case of the additive noise, the reconstruction accuracy of the shape of the surface of the distant object decreases with increasing steepness σ_ξ/l_ξ of the slopes of the roughnesses of its surface. It decreases with increasing the coefficient $\gamma_{n/s}$, which is equal to the ratio of the time-averaged intensity detected at the near-axial site of the image plane of the studied object in its absence to the time-averaged intensity in the image of this object at the same site in the absence of the additive noise. At the same time, as the distance from the axial site of the flat image of the object under study increases and its contour is approached, the reconstruction accuracy of the shape of the object surface by the contrast speckle pattern of this image decreases by approximately two times.

References

1. Horn B.K.P. *Robot Vision* (Cambridge, Massachusetts: MIT Press and New York: McGraw-Hill, 1986; Moscow: Mir, 1980).
2. Potapov A.A., Gulyaev Yu.V., Nikitov S.A., Pakhomov A.A., German V.A. *Noveishie metody obrabotki izobrazhenii* (The Newest Methods of Image Processing) (Moscow: Fizmatlit, 2008).
3. Troitsky I. *Proc. SPIE Int. Soc. Opt. Eng.*, **5203**, 1 (2003).
4. Mandrosov V.I. *Kvantovaya Elektron.*, **39**, 1059 (2009) [*Quantum Electron.*, **39**, 1059 (2009)].
5. Goodman J.W. *Statistical Optics* (New York: Wiley, 1985; Moscow: Mir, 1986).
6. Born M., Wolf E. *Principles of Optics* (London: Pergamon, 1970; Moscow: Nauka, 1973).
7. Bakut P.A., Mandrosov V.I., Matveev I.N., Ustinov N.D. *Teoriya kogerentnykh izobrazhenii* (Theory of Coherent Images) (Moscow: Radio i Svyaz', 1987).